

SUPPLEMENTARY INFORMATION

Calculation of the different chemical potentials

In this section we show how we estimate the different boundaries for the chemical potentials of the species involved, namely, oxygen, lithium and the halogens atoms that are needed to calculate the defects formation energies in Li_2O_2 .

Lithium: When the Li_2O_2 is formed at the cathode of the LAB under applied potential ϕ , the chemical potential of Li at the cathode is obtained as:

$$\mu_{\text{Li}} = \mu_{\text{Li}}^{\text{BCC}} - e\phi, \quad (\text{S1})$$

At open circuit conditions, it can be calculated as $\mu_{\text{Li}} = \frac{G(\text{Li}_2\text{O}_2)}{2} - \mu_{\text{O}}$, which is equivalent to take $\phi = \phi_{\text{eq}}$ in eq. (S1), with ϕ_{eq} the equilibrium potential of the LAB.

Following Freysoldt *et al.*,¹ we can calculate the top boundary for μ_{O} as will be shown next, so that this expression will give the minimum value for μ_{Li} .

Oxygen: In order to calculate $\mu(\text{O})$ we consider that the Li_2O_2 at the cathode is in equilibrium with gaseous O_2 , so that we set $\mu(\text{O}) = \mu(\text{O}_2) / 2$ in all the equations. To solve the problem of the well-known over-binding error of the DFT energy for the O_2 molecule, we employ the same approach of Radin and Siegel², in which the energy correction is obtained from the difference between the experimental heat of formation of Li_2O_2 and the calculated one. We then satisfy and solve the following set of equations:

$$\begin{aligned} 0 &= \Delta H_f^{\text{cal}}(\text{Li}_2\text{O}_2) - \Delta H_f^{\text{exp}}(\text{Li}_2\text{O}_2) \\ \Delta H_f^{\text{cal}}(\text{Li}_2\text{O}_2) &= E_s^{\text{DFT}}(\text{Li}_2\text{O}_2) - 2E_s^{\text{DFT}}(\text{Li}_{\text{BCC}}) - E_g^{\text{corr}}(\text{O}_2) \\ E_g^{\text{corr}}(\text{O}_2) &= E_s^{\text{DFT}}(\text{Li}_2\text{O}_2) - 2E_s^{\text{DFT}}(\text{Li}_{\text{BCC}}) - \Delta H_f^{\text{exp}}(\text{Li}_2\text{O}_2) \\ \mu(\text{O}_2) &= E_g^{\text{corr}}(\text{O}_2) + k_b T - TS_{\text{exp}} \end{aligned}$$

The subscripts *s* and *g* of the calculated total energies stand for the solid and gaseous phases, respectively. One can note that similar values of $\mu(\text{O})$ can be obtained if the heat of formation of water is considered³. It is also important to note that the calculated chemical potential used in Eq. 1 of the manuscript for the Formation Energy of a certain defect, is a theoretical energy value that must be consistent with the total energy (E_{T}) calculated for the solid under study, with and without defects. Naturally, these energy values strongly depend on the functional used. For instance, the total energies of pristine Li_2O_2 are -38.91 eV, -53.51 eV, -67.02 eV for the functionals PBE, HSE($\alpha=0.25$) and HSE($\alpha=0.48$), respectively. The theoretical chemical potential $\mu(\text{O})$ is calculated accordingly, obtaining -4.8 eV, -8.5 eV and -11.9 eV (at 300 K and 1 atm), using the corresponding functionals in each case. In this same order, we obtain a correction $\Delta[E_g^{\text{corr}}(\text{O}_2) - E_g(\text{O}_2)] = 0.74$ eV, 0.65 eV and 0.63 eV, respectively. In the case of Li BCC, the itinerant electrons do not generate much self-interaction errors, so that its total energy is rather insensitive to the HSE correction, as expected. The reported Formation energies in the manuscript are obtained with HSE($\alpha=0.48$), since it is the functional that better reproduces the band gap obtained with more sophisticated techniques as GW.

Halogens: The chemical potential of different halogen dopants in Li_2O_2 were calculated taking into account that there are three phases in equilibrium: Li_2O_2 (s), O_2 (g) and the reservoir of dopants, that in this case are the FLi, LiCl, BrLi and ILi salts. This gives three equations for each case (here exemplified for chlorine):

$$\begin{aligned} G(\text{Li}_2\text{O}_2) &= 2\mu_{\text{Li}} + 2\mu_{\text{O}} \\ G(\text{O}_2) &= 2\mu_{\text{O}} \\ G(\text{LiCl}) &= \mu_{\text{Li}} + \mu_{\text{Cl}} \end{aligned}$$

From which we get:

$$\mu_{\text{Cl}} = G(\text{LiCl}) - \frac{1}{2}G(\text{Li}_2\text{O}_2) - \frac{1}{2}G(\text{O}_2)$$

It is important to mention that, we consider also HSE with $\alpha = 0.48$ in all the simulations of these salts because, similarly as in Li_2O_2 , the calculated electronic gap gets closer to the experimental value, as can be observed in Table S1.

Table S1: Calculated and experimental values for LiF, LiCl, and LiBr using PBE and HSE with $\alpha = 0.25$ and 0.48 .

Band gap	PBE	$\alpha=0.25$ (eV)	$\alpha=0.48$(eV)	Exp.(eV)⁴
LiF	9.1	11.4	13.7	13.6
LiCl	5.7	7.0	8.5	9.4
LiBr	4.5	5.5	6.9	7.6

Summarizing, for P and T at ambient conditions and using HSE ($\alpha = 0.48$) we obtain $\mu_{\text{O}} = \mu(\text{O}_2)/2 = -11.9 \text{ eV}$, $\mu_{\text{Li}} = -1.9 \text{ eV}$, $\mu_{\text{F}} = -11.7 \text{ eV}$, $\mu_{\text{Cl}} = -7.9 \text{ eV}$, $\mu_{\text{Br}} = -6.6 \text{ eV}$ and $\mu_{\text{I}} = -4.87 \text{ eV}$.

Calculated Bader charges

In Table S2, we present the calculated Bader charges of the Li, O and halogens atoms obtained for the most energetically favored defect in each case. Although there is a slight difference in the calculated charge for each hallogen, it can be concluded that all of them are approximately in a valence state -1. In the same line, in all the cases the oxygen ion is approximately in a valence state -1 as expected for a peroxide crystal and the Lithium close to a valence state +1.

Table S2: Calculated Bader charges of the Li, O and halogens for the most energetically favored defect for each halogen.

atom	F ⁺ _{O2}	Cl ⁺ _{O2}	Br ⁺ _{O2}	I ⁺ _{O2}
Li	0,13	0,13	0,13	0,13
O	~6,85	~6,85	~6,85	~6,85
Halogen	7,88	7,85	7,82	7,76

Estimation of the the activation barrier of hole polarons

At variance with the Li vancancy, in the case of the hole polaron, it is mandatory to use HSE in the calculation of the activation barrier, E_a . Due to the huge computational demand of the NEB method using HSE, we estimate E_a of the hole polaron in the presence of the Cl dopant calculating the intermediate step in the diffusion paths, schematized in Figure S.1

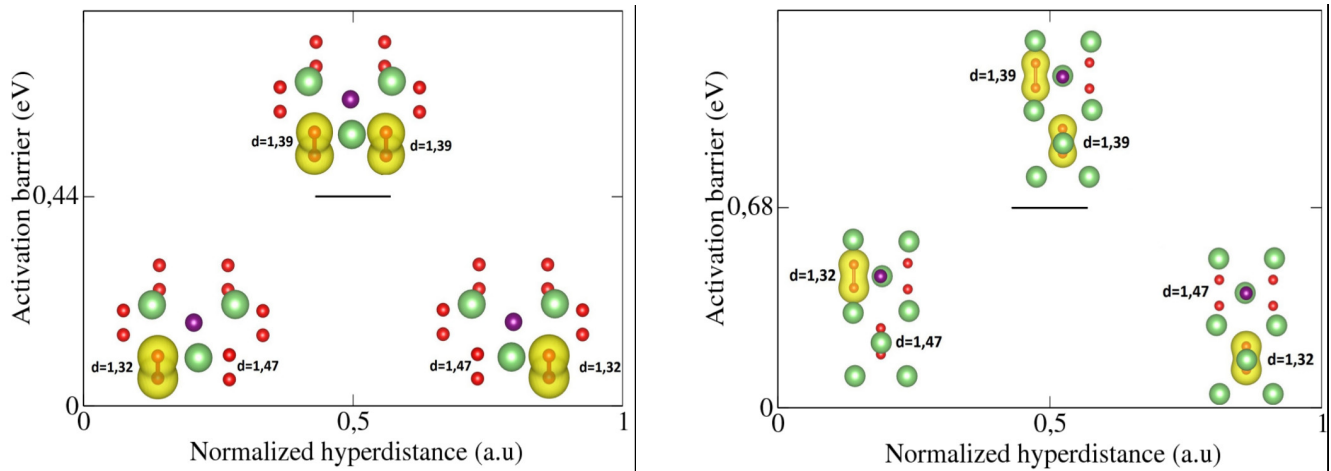


Figure S.1: Estimated E_a (in eV) for the intermediate step with respect to extreme cases, of the hole polaron hopping for the in-plane (left) and out of plane (right) diffusion paths. In yellow we schematized the charge density of each step at the dimers involved. At the intermediate step, the charge is distributed between two neighboring dimers. Red and green atoms represent Oxygen and Li, while violet is the halogen dopant.

Thermodynamic of the Li_2O_2 decomposition reaction

The reaction $2\text{Li}_2\text{O}_2(\text{s}) \leftrightarrow 2\text{Li}_2\text{O}(\text{s}) + \text{O}_2(\text{g})$ is not spontaneous under the conditions of operation of a LAB, that is, room temperature and partial pressure of oxygen 0.2 bar. However, it can become thermodynamically possible at low oxygen partial pressures.

In order to estimate the region of stability of the Li_2O_2 we calculate the Gibbs free energy of formation of the decomposition reaction by resorting to thermodynamic data available in literature,^{5,6} according to:

$$\Delta G^0 = 2\Delta G_f^0(\text{Li}_2\text{O}) + \Delta G_f^0(\text{O}_2) - 2\Delta G_f^0(\text{Li}_2\text{O}_2)$$

The calculated value is $G^\circ = 22.7 \text{ kJ/mol(O}_2\text{)}$. Therefore, the oxygen partial pressure at which the decomposition reaction becomes spontaneous at 25 °C is:

$$p_{\text{O}_2} = \exp(\Delta G^\circ / RT) \sim 10^{-4} \text{ bar}$$

That is, the decomposition of Li_2O_2 to form Li_2O is thermodynamically spontaneous at relatively moderate oxygen partial pressure. In any case, the kinetic aspect of this process needs to be considered further. Thus, Yao *et al.* [7] reported that a bulk sample of Li_2O_2 decomposed bellow 250-300 °C indicating that the kinetic play an important role.

Since the Li_2O_2 pristine deposit prepared by Nakanishi and collaborators,⁸ implied sample drying under vacuum, and the AFM analysis was performed in an Ar-filled glovebox, it is probably that the lithium peroxide decomposed partially, taking into account that the samples used during the AFM experiment are much thinner than in the LAB, namely around 20-30 nm or even less. More over, for these ultra-thin films the conduction mechanism is mainly tunneling and not diffusion, as expected in micro-metric samples.

References

- [1] Ch. Freysoldt, B. Grabowski, T. Hickel and J. Neugebauer, Review of Modern Physics, 2014, **86**, 253.
- [2] M. D. Radin and D. J. Siegel, Energy Environ. Sci., 2013, **8**, 2370.
- [3] F. Calle-Vallejo, J. I. Martínez, J. M. García-Lastra, M. Mogensen, & J. Rossmeisl. Angew. Chem. Int. Ed., 2010, 49, 7699.
- [4] R. T. Poole, J. G. Jenkin, J. Liesegang, and R. C. G. Leckey, Phys. Rev. B, 1975, **11**, 5179.
- [5] D. R. Lide (Ed.). Handbook of Chemistry and Physics, 76th Edition, CRC Press, 1995.
- [6] M. W. Chase (Ed.), JANAF Thermochemical Tables, 4th Edition, NIST, 1998.
- [7] P. C. Yao *et al.*, Journal of The Electrochemical Society, 2013, **160**, A824.
- [8] S. Matsuda, Y. Kubo, K. Uosaki, K. Hashimoto and S. Nakanishi, *J. Phys. Chem. C*, 2016, **120**, 13360–13365.